Res Chem Intermed (2014) 40:1483–1493
DOI 10.1007/s11164-013-1053-z

Effect of porosity of α-alumina on non-thermal plasma decomposition of ethylene in a dielectric-packed bed reactor

M. Sanjeeva Gandhi · Antony Ananth · Young Sun Mok · Jun-Ik Song · Kyu-Hyun Park

Received: 6 November 2012 / Accepted: 15 January 2013 / Published online: 29 January 2013

Abstract The performances of the porous and nonporous α-alumina (α-Al_2O_3) for the decomposition of ethylene in a dielectric-packed bed plasma reactor were comparatively examined with respect to the decomposition efficiency and the formation of byproducts. The decomposition was mainly controlled by discharge power, oxygen content, and properties of the alumina, such as porosity and surface area. The addition of a small quantity of oxygen led to an increase in the generation of oxidative species which eventually increased the ethylene decomposition efficiency. In the presence of 5 % oxygen, ethylene at an initial concentration of 1,898 ppm was completely oxidized into CO or CO_2 when using the porous α-alumina. On the other hand, the nonporous α-alumina resulted in an incomplete oxidation, producing several carbon-containing byproducts other than CO and CO_2. Moreover, with the other conditions kept constant, the decomposition efficiency obtained with the porous α-alumina was higher than that with the nonporous one, suggesting the adsorption capability of the packing material plays an important role in the decomposition process.

Keywords Dielectric-packed bed plasma reactor · Ethylene · α-Alumina · Porosity · Decomposition

Introduction

Ethylene is a colorless, sweet odor flammable gas which is classified as a volatile organic compound (VOC). The use of ethylene has been increasing gradually due to

M. S. Gandhi · A. Ananth · Y. S. Mok (✉)
Department of Chemical and Biological Engineering, Jeju National University, Jeju 690-756, Korea
e-mail: smokie@jejunu.ac.kr

J.-I. Song · K.-H. Park
National Institute of Animal Science, Rural Development Administration, Suwon 441-706, Korea

its huge demand for the production of polymers and other industrial chemicals. Ethylene itself is of low toxicity to humans and is unlikely to have any adverse human health effects, but the direct emission of this gas to the environment should be controlled to avoid secondary pollution. As a VOC, ethylene can be involved in photochemical reactions that produce ground level ozone, which affects human health and damages crops. Apart from the anthropogenic sources, ethylene is produced from natural sources, plants, and plant products. For example, fruits and vegetables emit ethylene as they ripen. It is well known that ethylene is responsible for the ripening and ageing process. Exposure to ethylene in their storage environment causes deterioration of fruits and vegetables, which becomes an economically important issue in agricultural industry. Therefore, it is important to remove ethylene from the storage environment to increase the storage life.

Recently, non-thermal plasma techniques have been widely used for environmental remediation [1, 2]. Many researchers found that non-thermal plasma system is a feasible technology that can effectively decompose VOCs of a wide concentration range. In non-thermal plasma processes for the decomposition of VOCs, the performance generally depends on the concentration of pollutant, flow rate, reactor temperature, operation voltage, and power input. In the case of the plasma reactor system containing packing material, the properties of the packing material such as surface area and porosity may also play an important role in the decomposition. Tsuru et al. [3] indicated the decomposition of methanol was dependent on the pore diameter of the packing material, and Van Durme et al. [4] reported that the VOC sorption on the surface of the packing material is one of the most critical factors for determining the decomposition efficiency, implying that a large surface area is desirable. On the other hand, Kim et al. [5] reported that the coating of metal oxide on the packing material was rather important than the surface area for the non-thermal plasma oxidation of toluene. Hassani et al. [6] have documented that toluene can completely be decomposed by adjusting the reaction temperature and the surface area of the packing material.

In this work, we investigated the effect of the porosity of the packing material on the decomposition of ethylene in a dielectric-packed bed plasma reactor. The packing materials used were porous and nonporous α-alumina. The input power and the oxygen content were chosen as additional experimental parameters.

Materials and methods

The dielectric-packed bed plasma reactor used for the decomposition of ethylene (hereafter, plasma reactor) is schematically represented in Fig. 1. Plasma was created inside a quartz tube whose inner and outer diameters were 21 and 25 mm, respectively. A high voltage electrode made of stainless steel (8-mm diameter) was fixed at the center of the quartz tube and the rest area was filled with 3-mm porous or non-porous α-alumina (Al_2O_3) pellets at an amount of 15 g. This setup was enclosed by another cylindrical case (acrylic material) filled with water for temperature maintenance and the ground connections to be made. The porous α-alumina was obtained from Sigma-Aldrich and the non-porous one from Daihan

Scientific. The Brunauer-Emmett-Teller (BET) surface areas of the porous and nonporous α-alumina were measured to be 348.3 and 1.53 $m^2\ g^{-1}$, respectively, by a BET surface area analyzer (AUTOSORB-1-MP, Quantachrome). In case of the porous α-alumina, the average pore radius and total pore volume were 28.6 Å and 0.450 $cm^3\ g^{-1}$, respectively. The dielectric constant of pure α-alumina was measured as a function of frequency in the range of 10 kHz–4 MHz as reported by Farag et al. [7], and found to be 9.4 at room temperature and frequency-independent. The first and second acidity constants of hydrated α-alumina have been reported to be $pK_1 = 7.06$ and $pK_2 = 11.06$ at 25 °C [8]. For comparison, a separate ethylene decomposition experiment was carried out by using 3-mm porous β-zeolite (Cosmo Fine Chemical; BET surface area: 550 $m^2\ g^{-1}$) as a packing material.

The feed gas was composed of ethylene (1,898 ppm), oxygen (0–8 % by volume) and nitrogen as a diluent. The total flow rate was maintained at 1.0 L min^{-1} by using mass flow controllers (MKS Instruments, USA). A high voltage AC power in the range of 10–16 kV at a frequency of 400 Hz was applied to the stainless steel electrode acting as the discharging electrode. The decomposition efficiency was examined by varying the input power up to 100 W. The input power was measured by a digital power meter (Model WT200; Yokogawa). A Fourier transform infrared (FTIR) spectrometer (Bruker IFS 66/S; Germany) was employed to analyze the decomposition efficiency of the ethylene. The ethylene and the destruction products were assigned in the spectra and the absorbance was converted into concentration using standard procedures [9]. The decomposition efficiency was calculated by $100 \times (C_0 - C)/C_0$, where C_0 and C are the concentrations at the inlet and outlet of the reactor, respectively. The discharge power was measured by using the Lissajous curve generated in the oscilloscope (Tektronix MSO/DPO3000).

The morphological structure of the α-alumina was characterized by a field emission scanning electron microscope (FESEM; JEM1200EX II, JEOL). The porous alumina exhibited an uneven surface with many micro-pores (Fig. 2a), whereas the nonporous alumina displayed a smooth surface morphology (Fig. 2b). In the absence of oxygen, a polymer-like solid deposit was formed inside the reactor

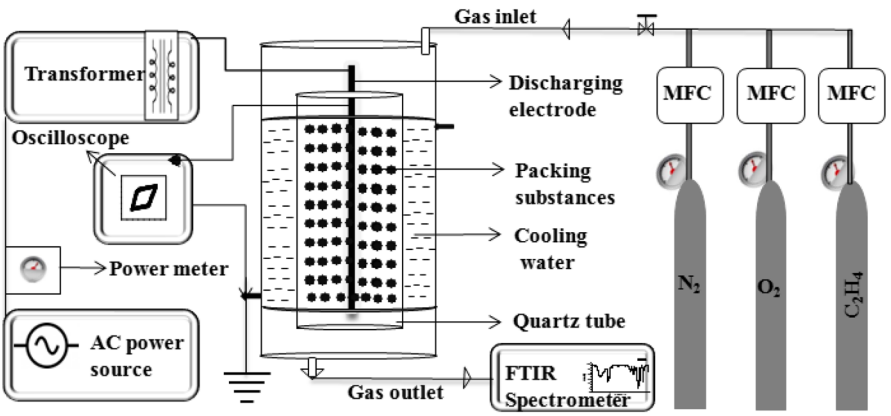

Fig. 1 Schematic diagram of the experimental setup

wall and on the surface of alumina pellets. In order to identify the polymer-like complex, the deposit was mixed with KBr, and then analyzed by the FTIR spectrometer. The deposit was also analyzed by a Gas Chromatograph-Mass Spectrometer (GC–MS; QP2010Plus; Shimadzu) after dissolving it in ethanol.

Results and discussions

The relationship between the input power and the discharge power is shown in Fig. 3 for four different cases, i.e., no packing material, nonporous α-alumina, porous α-alumina, and porous silica. The discharge power of the plasma reactor containing the porous or the nonporous α-alumina was significantly higher than that without packing material. This might be due to the fact that the presence of the packing material in effect increases the average electric field intensity, resulting in reducing the discharge ignition voltage. Compared to the nonporous α-alumina, the porous α-alumina exhibited higher discharge powers at all input powers, which can be explained by numerous micro-discharges occurring in the micro-pores of the porous α-alumina. The generation of plasma in the micro-pores can also contribute to the decomposition of ethylene when it diffuses in through the pores.

Decomposition efficiency and by-products distribution

Figure 4 shows the ethylene decomposition efficiencies obtained with the porous (a) and the nonporous α-alumina (b) as functions of the input power and the oxygen content. In both cases, the decomposition efficiency increased with increasing the input power and the oxygen content. It was found that the decomposition efficiency with the porous α-alumina was a lot higher than that with the nonporous one at all input powers explored. When using the porous α-alumina, complete decomposition was achieved at 45 W with the oxygen content of 5 %. But, when the nonporous α-alumina was used, only 62.5 % was decomposed at the same input power of 45 W, and this had to be increased to 80 W for complete decomposition.

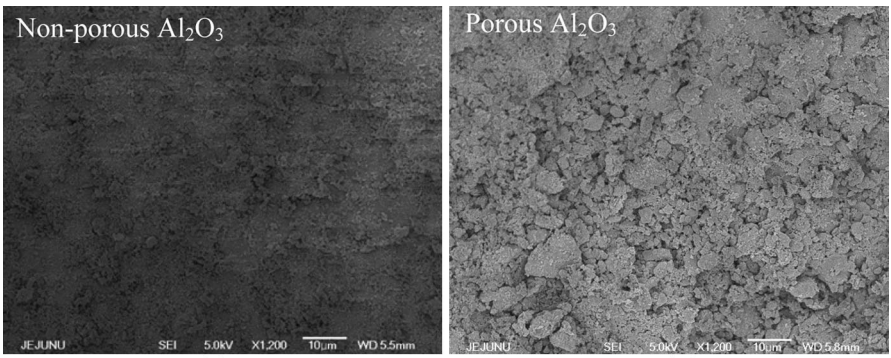

Fig. 2 FESEM surface morphological images of the porous and nonporous α-Al_2O_3

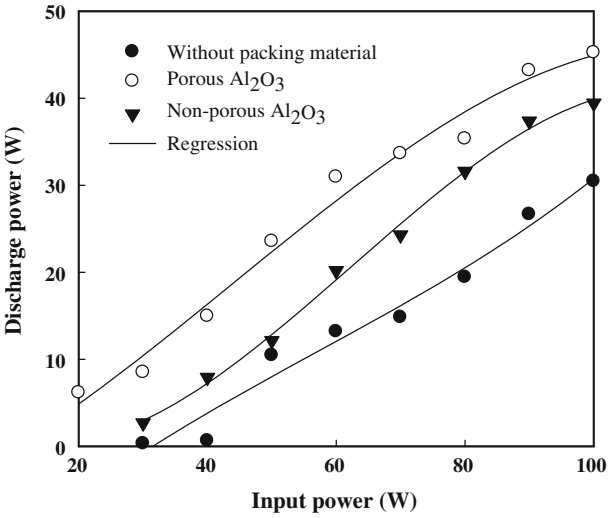

Fig. 3 Input powers versus discharge power

According to Reddy et al. [10], who investigated the decomposition of H_2S using a catalytic-packed bed plasma reactor, packing length affects the decomposition performance because of a change in the discharge volume and also because of a sulfur deposit over the catalyst surface. But the results in Fig. 4 cannot be explained by the packing length because the packing lengths for the porous and non-porous α-alumina were nearly the same. The enhanced decomposition of the ethylene with the porous α-alumina may be ascribed to the adsorption effect and the numerous micro-discharges generated in the micro-pores. As shown above, the discharge power of the plasma reactor packed with the porous α-alumina was higher than that with the nonporous one; therefore, it is natural that the decomposition efficiency with the porous α-alumina should be higher. Besides, the porous α-alumina possesses a large specific surface area and adsorption capability. The active sites of the porous α-alumina pave the way for the adsorption of ethylene and other reactive species generated by the plasma before reacting with each other. Rousseau et al. [11] reported that the porosity of the catalyst favors the adsorption of highly oxidative radicals such as atomic oxygen as well as pre-concentrated VOC on its surface. The adsorbed ethylene can easily react with the reactive species to be decomposed. Note that molecules in the gas phase are randomly moving at very high speed, whereas those adsorbed on the surface of solids can only vibrate about their fixed positions. In other words, molecules fixed on the surface by adsorption can be more easily attacked by the reactive species generated by the plasma than those in the gas phase. Thus, the presence of an adsorbent in the plasma reactor can enhance the rate of decomposition which is relatively slow in the gas phase. Furthermore, when the porous α-alumina was exposed to plasma, it may induce the formation of additional charge carrier trap sites which would extend the lifetime of the charge carriers [12], thereby increasing the decomposition via reactions with charged species. In this context, it stands to reason that the porous α-alumina having

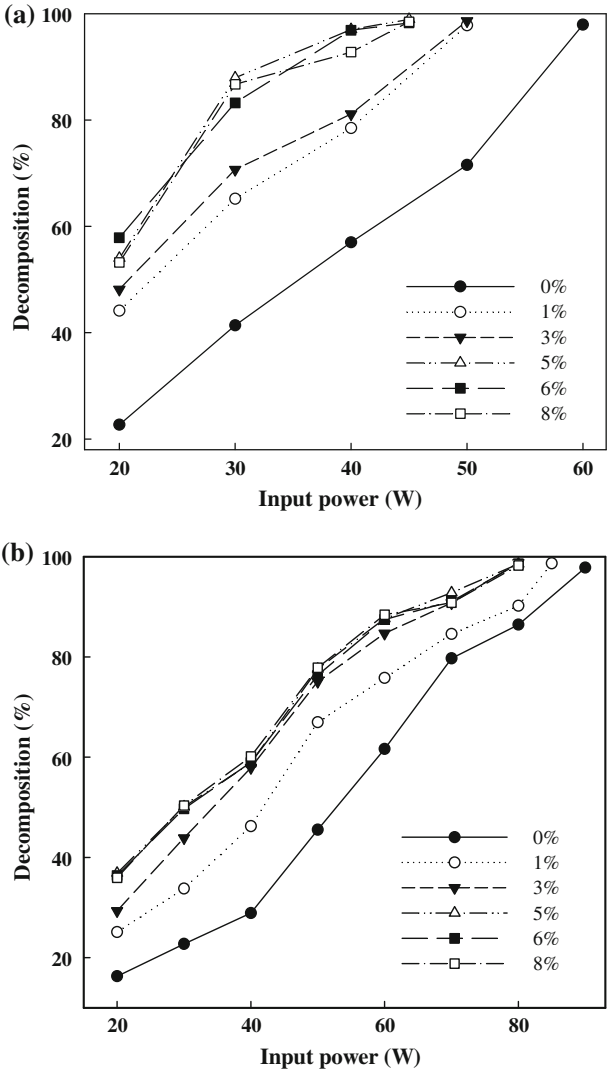

Fig. 4 Decomposition of ethylene as a function of the oxygen content over the porous (**a**) and the nonporous α-Al_2O_3 (**b**)

a large surface area exhibited better activity than the non-porous one. After the decomposition, the products such as CO and CO_2 diffuse out through the micropores. Meanwhile, the decomposition efficiency significantly increased with increasing the oxygen content up to 5 % and was then saturated at higher oxygen content. When nitrogen alone was used, the ethylene decomposition was noticeably lower than that in the presence of oxygen. In the absence of oxygen, reactive species are responsible for the decomposition which is generated only from the nitrogen. On the other hand, when oxygen coexists, reactive species originated from both

nitrogen and oxygen can contribute to the decomposition of ethylene. Moreover, fragments resulting from collisions between ethylene and reactive species like excited N_2 can be scavenged by oxidative radicals such as atomic oxygen and ozone, speeding up the fragmentation reactions of ethylene. A similar tendency was observed by Kim et al. [13] for the effect of oxygen on the decomposition of toluene in a catalyst-packed bed plasma reactor.

A comparison of the ethylene decomposition efficiencies between the porous and nonporous packing materials is presented in Fig. 5 as a function of input power. As observed, the porous α-alumina and β-zeolite resulted in higher decomposition efficiencies than the non-porous packing material due to the aforementioned reasons. The porous β-zeolite exhibited similar decomposition efficiency to the porous α-alumina. The results in Fig. 5 again confirm that it is necessary to use porous packing material to facilitate the decomposition.

Figure 6 shows the behavior of byproducts formation as a function of the oxygen content when the porous (a) and the nonporous α-alumina (b) were used. The influence of the oxygen content on the distribution of byproducts with the porous α-alumina was different from that with the nonporous one. The byproducts identified included CO_x (CO and CO_2), acetylene, methane, and nitrous oxide (N_2O). The results clearly indicate that an increase in the oxygen content reduced the formation of acetylene and methane. Especially, when the porous α-alumina was used, acetylene and methane completely disappeared at oxygen contents above 5 %. In contrast, significant amounts of the aforementioned species were retained in the nonporous α-alumina case, even at an oxygen content as high as 8 %. Further, with the nonporous α-alumina, formaldehyde and acetaldehyde were also detected in the FTIR spectra as additional byproducts (Fig. 7). In both cases, the N_2O concentration gradually increased with the increase of oxygen content. Comparison of the results

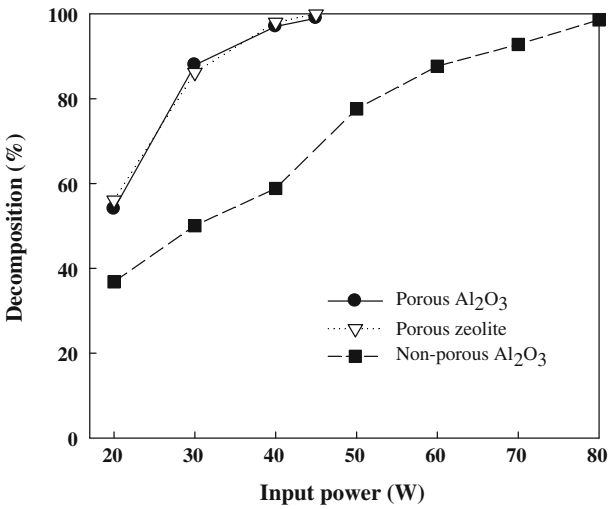

Fig. 5 Comparison of decomposition efficiencies between the porous and nonporous packing materials (oxygen content: 5 %)

obtained with the porous and nonporous alumina clearly shows that the porous structure with a high specific surface area is more desirable.

GC–MS and FTIR study of the polymer deposition

The color of α-alumina was changed from white to brownish yellow under the non-oxidative condition, i.e., in the absence of oxygen. In addition, some brownish yellow polymer-like deposition was also noticed on the reactor wall. In Fig. 8, the FTIR spectrum shows that the vibrational regions correspond to the polymer-like

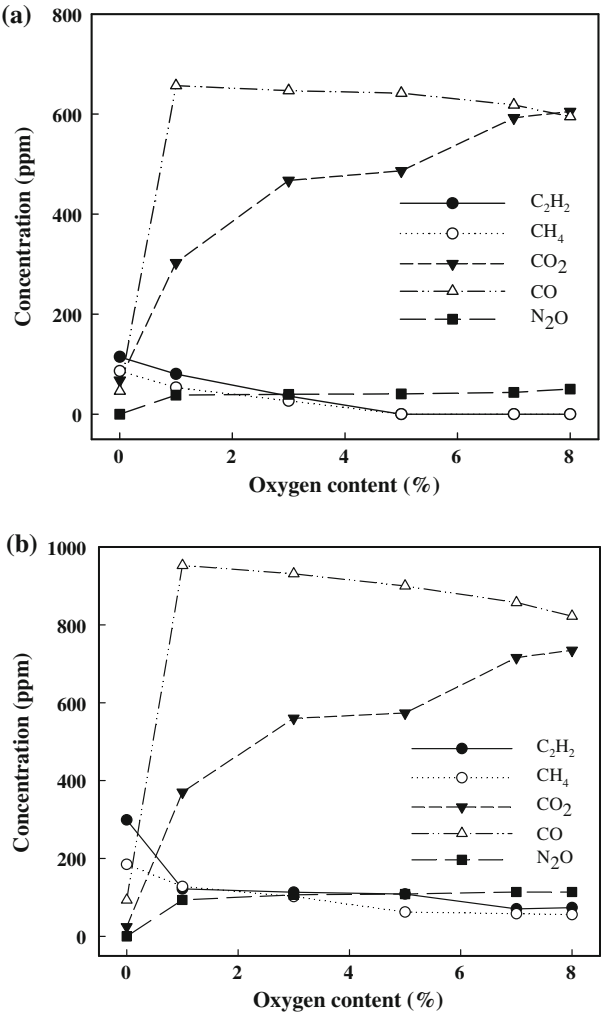

Fig. 6 Distribution of byproducts as a function of the oxygen content. **a** With the porous α-Al_2O_3 at 40 W. **b** With the nonporous α-Al_2O_3 at 80 W

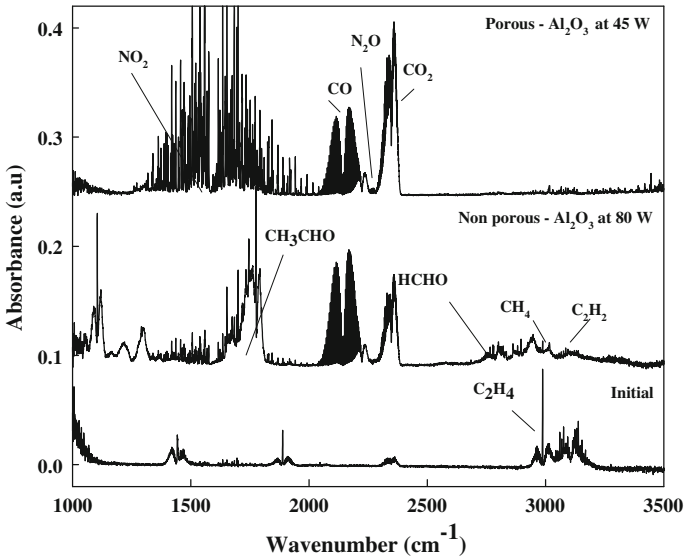

Fig. 7 FTIR spectra of the effluent gas before and after the plasma treatment

deposits containing axial deformation of C–H at 2,876 cm^{-1} (CH_3 symmetric), 2,928 cm^{-1} (CH_2 symmetric), and 2,963 cm^{-1} (CH_3 symmetric), angular deformations of C–H at 1,456 cm^{-1}(CH_3 asymmetric) and 1,377 cm^{-1}(CH_3 symmetric), and axial deformation of C=C at 1,647 cm^{-1} [14]. The peak at 1,028–1,099 cm^{-1} ascribed to C–O stretching vibrations corresponds to the carbonyl and carboxyl groups and the sharp peak around 1,264 cm^{-1} is due to the C–H bond, all of which represent the presence of poly-hydrocarbon. An important characteristic peak of ethylene copolymers was observed at a wave number of 803 cm^{-1} [15]. Furthermore, the GC–MS results in Fig. 9 also confirmed the deposition of various poly-hydrocarbons on the surface of the reactor wall. As per the report by Ognier et al. [16], nitrogen molecules (without oxygen) play major roles in the polymerization process through the formation of several chemical bonds.

Figure 10 shows the FTIR spectra of the porous α-alumina before and after the plasma treatment in the absence of oxygen. The smooth peak in the region from 400 to 1,017 cm^{-1} was attributed to the stretching vibration of the Al–O–Al bond. As per the report by Costa et al. [17], the broadening of this peak is due to the allocation of a vacancy between the octahedral and tetrahedral sites. The peak around 3,400 cm^{-1} represents the stretching mode of the O–H bond. However, the sharp peak at 1,625 cm^{-1} indicates the CH linkage with Al_2O_3 (Al–CH_3 deformation mode) [18]. The high intensity of C–H peak indicates the interaction of α-alumina with methyl groups of the ethylene decomposition products. Comparing the two spectra in Fig. 10, the resonance peak of O–H at 1,625 cm^{-1} slightly increased after the plasma treatment, which suggests that the porous α-alumina absorb some amounts of OH during the plasma decomposition process.

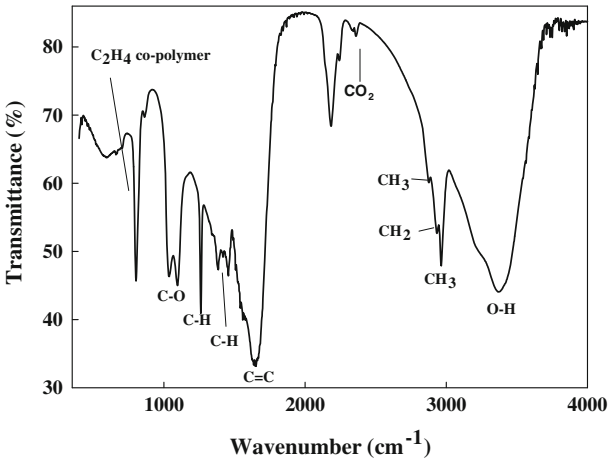

Fig. 8 FTIR spectrum of the polymer-like deposits on the reactor wall under non-oxidative condition

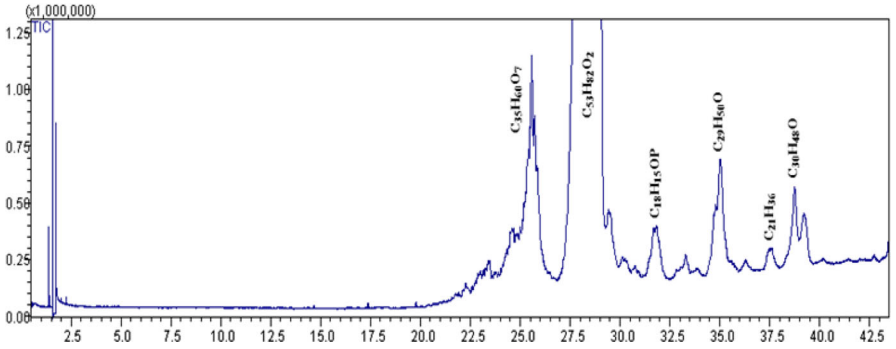

Fig. 9 GC-MS spectrum of the polymer-like deposits on the reactor wall under non-oxidative condition

Conclusions

The effect of parameters such as input power and oxygen content on the ethylene decomposition was investigated with a plasma reactor packed with the porous or the nonporous α-alumina. The decomposition efficiency increased greatly with an increase in the oxygen content up to 5 % and was then saturated at higher oxygen content. The decomposition efficiency for the porous α-alumina was found to be much higher than for the nonporous one, which can be explained by the surface area and porosity effect. Complete decomposition was achieved at an input power of 45 W and an oxygen content of 5 % with the porous α-alumina, whereas 80 W was required with the nonporous α-alumina. Moreover, the nonporous α-alumina packing material resulted in an incomplete oxidation, producing several carbon-containing byproducts other than CO_2 and CO. With the porous α-alumina, formation of acetylene, methane, and acetaldehyde was completely avoided and the production of CO_2 instead of CO was greatly enhanced. When oxygen was not

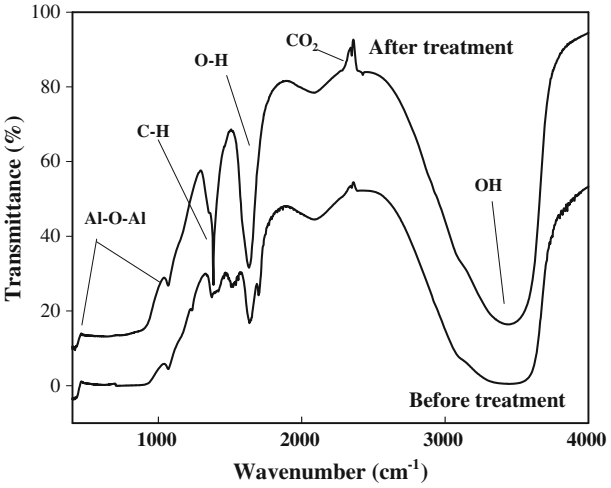

Fig. 10 FTIR spectra of the porous α-Al_2O_3 before and after the plasma treatment in the absence of oxygen

added to the feed gas, brownish yellow solid deposits were formed on the surface of the α-alumina pellets and inside the reactor. The FTIR and GC–MS characterization of the solid deposits indicated the presence of various polymer-like products.

Acknowledgment This work was carried out with the support of "Cooperative Research Program for Agriculture Science & Technology Development (Project No. PJ008508032012)", Rural Development Administration, Republic of Korea.

References

1. C.H. Wang, Y. Wu, G.F. Li, J. Electrostat. **66**, 71 (2008)
2. Y.P. Zhang, Y. Li, Y. Wang, C.J. Liu, B. Eliasson, Fuel. Proc. Technol. **83**, 101 (2003)
3. T. Tsuru, T. Kan-no, T. Yoshioka, M. Asaeda, J. Membr. Sci. **280**, 156 (2006)
4. J. Van Durme, J. Dewulf, K. Demeestere, C. Leys, H.V. Langenhove, Appl. Catal. B **87**, 78 (2009)
5. S.C. Kim, J. Hazard. Mater. **91**, 285 (2002)
6. A. Hassani, M. Keyvanfar, A. Hassani, Aust. J. Basic Appl. Sci. **5**, 1738 (2011)
7. I.S.A. Farag, I.K. Battisha, M.M. El-Rafaay, Indian J. Pure Appl. Phys. **43**, 446 (2005)
8. W.E. Halter, Geochim. Cosmochim. Acta **63**, 3077 (1999)
9. P.L. Hanst, S.T. Hanst, *Procedures in Infrared Analysis of Gases* (Infrared Analysis, Anaheim, 1993)
10. E.L. Reddy, J. Karuppiah, V.M. Biju, C. Subrahmanyam, Int. J. Energy Res. (2012). doi: 10.1002/er.2924
11. A. Rousseau, O. Guaitella, J. Ropcke, L.V. Gatilova, Y.A. Tolmachev, Appl. Phys. Lett. **85**, 2199 (2004)
12. P.F. Ambrico, M. Ambrico, A. Colaianni, L. Schiavulli, G. Dilecce, S.D. Benedictis, J. Phys. D **43**, 325201 (2010)
13. H.H. Kim, A. Ogata, S. Futamura, Appl. Catal. B **79**, 356 (2008)
14. C.A. Caceres, L. Zborowski, S.V. Canevarolo, Mat. Res. **14**, 569 (2011)
15. A.J. Choudhury, H. Kakati, A.R. Pal, D.S. Patil, J. Chutia, J. Phy. Chem. Solids **208**, 1 (2010)
16. S. Ognier, S. Cavadias, J. Amouroux, Plasma Proc. Polym. **4**, 528 (2007)
17. T.M.H. Costa, M.R. Gallas, E.V. Benvenutti, J.A.H. da Jornada, J. Phys. Chem. B **103**, 4278 (1999)
18. J.D. Ferguson, A.W. Weimer, S.M. George, Chem. Mater. **16**, 5602 (2004)